ISSN: 0975-8585

Research Journal of Pharmaceutical, Biological and Chemical Sciences

Experimental and Theoretical Investigation of 5-(azidomethyl)quinolin-8-ol as a Corrosion Inhibitor for Carbon Steel in Hydrochloric Acid Medium.

H Tayebi[1], B Himmi[4], Y Ramli[3], A Zarrouk[2]*, A Geunbour[1], A Bellaouchou[1], H Zarrok[5], M Boudalia[1], and A El Assyry[6].

[1]Laboratoire Nanomatériaux, Nanotechnologies et Environnement, Faculté des Sciences, Université Mohamed V, BP. 1014 Rabat, Morocco.
[2]LCAE-URAC 18, Faculty of Science, First Mohammed University, PO Box 717, 60 000 Oujda, Morocco.
[3]Laboratoire de Chimie Thérapeutique, Faculté de Médecine et de Pharmacie de rabat, Université Mohamed V, BP 6203, Rabat, Morocco.
[4]Filière Techniques de Santé, Institut Supérieur des Professions Infirmières et Techniques de Santé, Avenue Hassan II - Km 4,5 Route Rabat-Casa, Rabat, Morocco.
[5]Laboratory Separation Processes, Faculty of Science, University Ibn Tofail PO Box 242, Kenitra, Morocco.
[6]Laboratoire d'Optoélectronique et de Physico-chimie des Matériaux (Unité associée au CNRST), Département de Physique,Université Ibn Tofail, B.P. 133, Kénitra, Maroc.

ABSTRACT

The inhibition effect of 5-(azidomethyl)quinolin-8-ol (QIN2) on the corrosion of carbon steel in 1.0 M HCl solution was investigated using electrochemical measurement and Density functional theory (DFT) at different concentrations and temperature. The corrosion inhibition efficiency increased with increase in inhibitor concentration, but decreased with increase in temperature. The polarization curves indicated that QIN2 behaved as a anodic-type inhibitor while the Nyquist plots revealed that the corrosion was a charge transfer controlled process. The adsorption of QIN2 takes place according to Langmuir's adsorption isotherm. Thermodynamic parameters were calculated and discussued. The quantum chemical calculations were applied to elucidate adsorption pattern of inhibitor molecules on steel surface.

Keywords: Carbon steel, Corrosion, EIS, Polarisation, DFT.

Corresponding author

ISSN: 0975-8585

INTRODUCTION

The major problem of carbon steel is its dissolution in acidic medium, Corrosion of steel in acidic aqueous solutions is one of the major areas of concern in many industries where in acids are widely used for applications such as acid pickling, acid cleaning, acid descaling, and oil well acidizing. Because of general aggressiveness of acid solution the materials of construction are getting corroded easily. Steel corrosion is a thermodynamically feasible process as it is associated with decrease in Gibb's free energy. Corrosion is an afflicting problem associated with every use of metals. The damage by corrosion results in high cost for maintenance and protection of materials used.

Development of methods to control corrosion is a challenge to scientists working in this area. Amongst various methods developed for corrosion protection, use of inhibitor is an attractive and most practical method for the protection of metals in contact with corrosion medium. Inhibitors reduce the corrosion of metallic materials by controlling the metal dissolution and consumption. Majority of the well-known inhibitors for the corrosion of steel in acidic medium are the organic compounds containing nitrogen, sulphur, oxygen atoms, or N-hetero cyclic compounds with polar groups. A large number of scientific studies have been devoted to the subject of corrosion inhibitors for carbon steel in acidic media [1-25].

The present investigation focuses on the use 5-(azidomethyl)quinolin-8-ol as corrosion inhibitor for steel metal in acidic medium using electrochemical methods and quantum chemical studies. 5-(azidomethyl)quinolin-8-ol contain some nitrogen and oxygen heteroatoms and an aromatic pyridine and benzene rings which act as major adsorption centers. Figure 1 show the molecular structures of the compound utilised in this investigation.

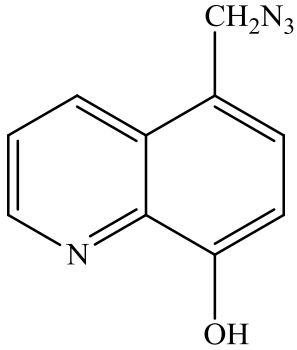

Figure 1 : 5-(azidomethyl)quinolin-8-ol (QIN2)

EXPERIMENTAL METHODS

Materials

The steel used in this study is a carbon steel (CS) (Euronorm: C35E carbon steel and US specification: SAE 1035) with a chemical composition (in wt%) of 0.370 % C, 0.230 % Si, 0.680 % Mn, 0.016 % S, 0.077 % Cr, 0.011 % Ti, 0.059 % Ni, 0.009 % Co, 0.160 % Cu and the remainder iron (Fe).

Solutions

The aggressive solutions of 1.0 M HCl were prepared by dilution of analytical grade 37% HCl with distilled water. The concentration range of (QIN2) used was 10^{-6} M to 10^{-3} M.

Polarization measurements

Electrochemical impedance spectroscopy

The electrochemical measurements were carried out using Volta lab (Tacussel- Radiometer PGZ 100) potentiostate and controlled by Tacussel corrosion analysis software model (Voltamaster 4) at under static condition. The corrosion cell used had three electrodes. The reference electrode was a saturated calomel

electrode (SCE). A platinum electrode was used as auxiliary electrode of surface area of 1 cm^2. The working electrode was carbon steel. All potentials given in this study were referred to this reference electrode. The working electrode was immersed in test solution for 30 minutes to a establish steady state open circuit potential (*E*ocp). After measuring the *E*ocp, the electrochemical measurements were performed. All electrochemical tests have been performed in aerated solutions at 303 K. The EIS experiments were conducted in the frequency range with high limit of 100 kHz and different low limit 0.1 Hz at open circuit potential, with 10 points per decade, at the rest potential, after 30 min of acid immersion, by applying 10 mV ac voltage peak-to-peak. Nyquist plots were made from these experiments. The best semicircle can be fit through the data points in the Nyquist plot using a non-linear least square fit so as to give the intersections with the *x*-axis.
The inhibition efficiency of the inhibitor was calculated from the charge transfer resistance values using the following equation:

$$\eta_z\% = \frac{R_{ct}^{i} - R_{ct}^{\circ}}{R_{ct}^{i}} \times 100 \quad (1)$$

where, R_{ct}° and R_{ct}^{i} are the charge transfer resistance in absence and in presence of inhibitor, respectively.

Potentiodynamic polarization

The electrochemical behaviour of carbon steel sample in inhibited and uninhibited solution was studied by recording anodic and cathodic potentiodynamic polarization curves. Measurements were performed in the 1.0 M HCl solution containing different concentrations of the tested inhibitor by changing the electrode potential automatically from -800 to 0 mV versus corrosion potential at a scan rate of 1 mV s^{-1}. The linear Tafel segments of anodic and cathodic curves were extrapolated to corrosion potential to obtain corrosion current densities (I_{corr}). From the polarization curves obtained, the corrosion current (I_{corr}) was calculated by curve fitting using the equation:

$$I = I_{corr}\left[exp\left(\frac{2.3\Delta E}{\beta_a}\right) - exp\left(\frac{2.3\Delta E}{\beta_c}\right)\right] \quad (2)$$

β_a and β_c are the anodic and cathodic Tafel slopes and ΔE is E-E_{corr}.

The inhibition efficiency was evaluated from the measured I_{corr} values using the relationship:

$$\eta_{Tafel}\% = \frac{I_{corr}^{\circ} - I_{corr}^{i}}{I_{corr}^{\circ}} \times 100 \quad (3)$$

where, I_{corr}° and I_{corr}^{i} are the corrosion current density in absence and presence of inhibitor, respectively.

Computational procedures

Density Functional theory (DFT) has been recently used [26-29] to describe the interaction between the inhibitor molecule and the surface as well as the properties of these inhibitors concerning their reactivity. The molecular band gap was computed as the first vertical electronic excitation energy from the ground state using the time-dependent density functional theory (TD-DFT) approach as implemented in Gaussian 03 [30]. For these seek, some molecular descriptors, such as HOMO and LUMO energy values, frontier orbital energy gap, molecular dipole moment, were calculated using the DFT method and have been used to understand the properties and activity of the newly prepared compounds and to help in the explanation of the experimental data obtained for the corrosion process.

ISSN: 0975-8585

RESULT AND DISCUSSION

Potentiodynamic Polarization measurements

The representative polarization curves for carbon steel in 1.0 HCl solution with QIN2 at different concentrations was shown in Fig. 2. In order to obtain information about the kinetics of the corrosion, some electrochemical parameters, i.e., corrosion potential (E_{corr}), corrosion current density (I_{corr}), andoic and cathodic tafel slopes (β_a, β_c) and the inhibition efficiency (η_{Tafel}) obtained from the polarization measurements were listed in Table 1.

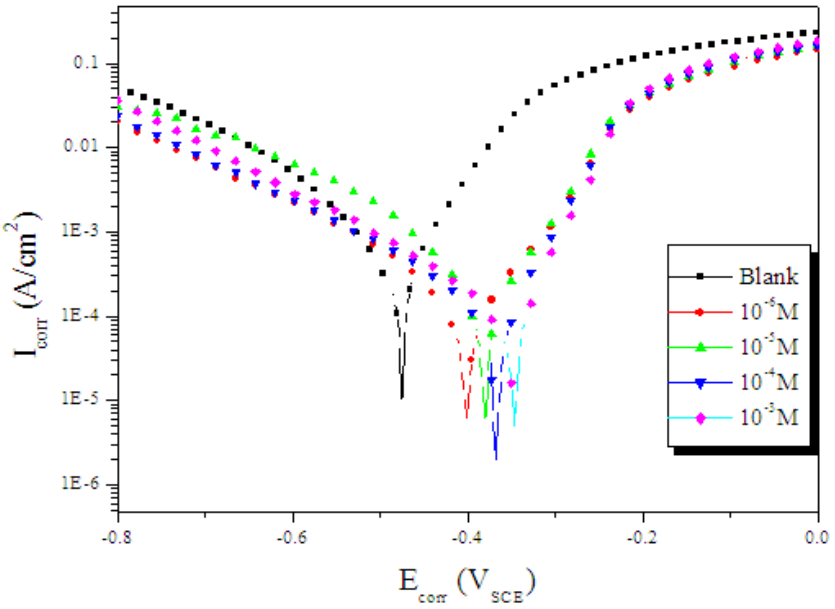

Figure 2 : Polarization curves for carbon steel in 1.0 HCl with different concentrations of QIN2.

From Tbale 1 and Figure 2 It was observed The reduction in I_{corr} is pronounced more and more with the increasing inhibitor concentration. It has been observed that 10^{-3} M of QIN2 serves as an optimum concentration that exhibit higher efficiency of corrosion inhibition. The increased inhibition efficiency with the inhibitor concentration indicates that the tested organic compound acts by adsorbing on the carbon steel surface. The cathodic branch of polarization curves was given rise to parallel lines. This shows that the addition of QIN2 to the 1.0 M HCl solution does not change the cathodic hydrogen evolution mechanism and the decrease of H^+ ions on the surface of carbon steel take place mainly through a charge transfer mechanism. There was measurable positive shift in corrosion potential (E_{corr}) after the addition of inhibitor. According to Li et al [31], if the displacement in corrosion potential is more than ±85 mV with respect to corrosion potential of the blank, then the inhibitor can be considered distinctively as a cathodic or anodic type. However, the maximum displacement in the present investigations for carbon steel in hydrochloric acid was more than that of 85mV, towards the positive direction. This observation suggests that constituents of inhibitor molecule may act as anodic type and brings the anodic reaction under control.

Table 1 : Potentiodynamic electrochemical parameters for the corrosion of carbon steel in 1.0 M HCl solution in the absence and presence of the investigated inhibitor at 303 K.

Inhibitor	Conc (M)	$-E_{corr}$ (mV_{SCE})	$-\beta_c$ (mV/dec)	I_{corr} ($\mu A\ cm^{-2}$)	η_{Tafel} (%)
Blank	1.0	477	138	579.0	-----
QIN2	10^{-6}	398	145	94.6	83.7
	10^{-5}	372	120	77.0	86.7
	10^{-4}	370	108	57.0	90.2
	10^{-3}	346	104	43.1	92.5

ISSN: 0975-8585

Electrochemical Impedance Spectroscopy Measurements

Effect of concentration

Figure 3 shows the Nyquist diagrams of carbon steel in 1.0 M HCl solutions containing different concentrations of QIN2 at 303 K. All the impedance spectra exhibit one single depressed semicircle.

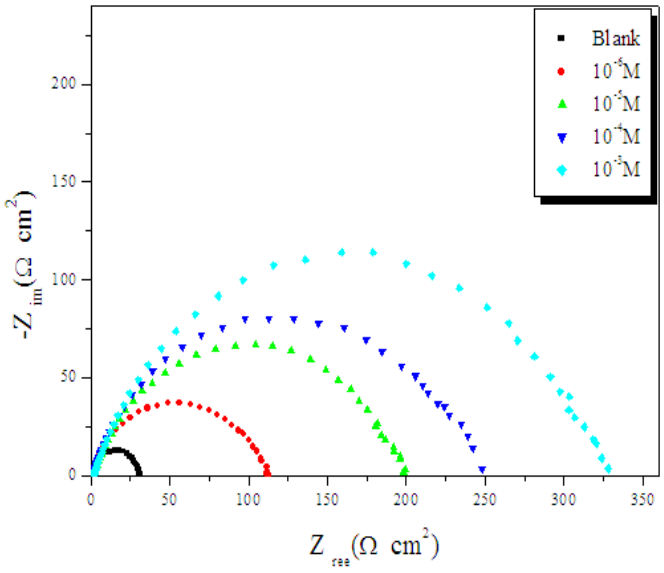

Figure 3: The Nyquist plots for corrosion of carbon steel in 1.0 M HCl in the absence and presence of different concentrations of QIN2 at 303 K.

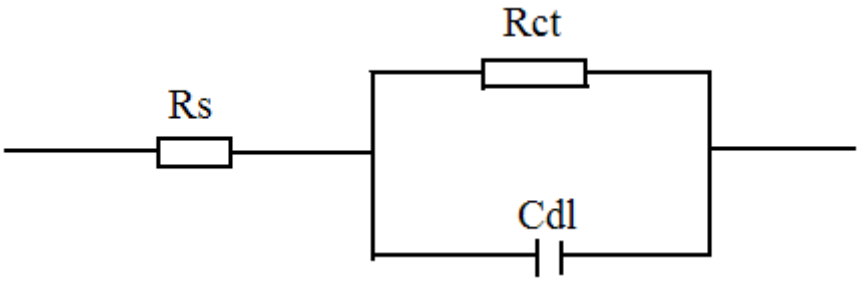

Figure 4 : Electrical equivalent circuit used to fit the impedance data.

The diameter of semicircle increases with the increase of QIN2 concentration. The impedance spectra exhibit one single capacitive loop, which indicates that the corrosion of steel is mainly controlled by a charge transfer process and the presence of QIN2 does not change the mechanism of carbon steel dissolution [32]. In addition, these Nyquist diagrams are not perfect semicircles in 1.0 M HCl that can be attributed to the frequency dispersion effect as a result of the roughness and inhomogeneous of electrode surface [33]. Furthermore, the diameter of the capacitive loop in the presence of inhibitor is larger than that in the absence of inhibitor (blank solution), and increased with the inhibitor concentration. This indicates that the impedance of inhibited substrate increased with the inhibitor concentration. This behavior is usually attributed to the inhomogeneity of the metal surface arising from surface roughness or interfacial phenomena [34], which is typical for solid metal electrodes [35]. Generally, when a non-ideal frequency response is presented, it is commonly accepted to employ the distributed circuit elements in the equivalent circuits. What is most widely used is the constant phase element (CPE), which has a non-integer power dependence on the frequency [36]. Thus, the equivalent circuit depicted in Figure 4 is employed to analyze the impedance spectra, where R_s represents the solution resistance, R_{ct} denotes the charge-transfer resistance, and C_{dl} represents the interfacial capacitance. The values of the interfacial capacitance C_{dl} can be calculated from equation 4:

$$C_{dl} = \frac{1}{2\pi f_{max} R_{ct}} \quad (4)$$

Where f is the maximum frequency. , values of the parameters such as Rs Rct, through EIS fitting as well as the derived paramaters Cdl and η_{Tafel} are listed in Table 2.

Table 2 : Electrochemical impedance parameters for carbon steel in 1.0 M HCl containing different concentrations of QIN2.

	Conc (M)	R_{ct} (Ω cm^2)	C_{dl} (μF/cm^2)	f_{max} (Hz)	η_z (%)	θ
Blank	1.0	31	128	40.0	---	-----
QIN3	10^{-6}	112	35.5	40	72.3	0.723
	10^{-5}	200	15.9	50	84.5	0.845
	10^{-4}	250	10.1	63	87.6	0.876
	10^{-3}	327	9.7	50	90.5	0.905

Effect of temperature

Temperature is an important parameter in the studies of metal dissolution. The effect of temperature on the inhibited acid-metal reaction is very complex because many changes may occur on the metal surface such as rapid etching, desorption of inhibitor and the inhibitor may undergo decomposition. Figures 5 and 6 shows Nyquist Impedance plots for carbon steel in 1.0 M HCl in the absence and the presence of 10^{-3} M QIN2 at different temperatures. As seen, increasing the temperature decreases the size of the depressed semicircles indicating increase of the corrosion rate (reciprocal of the charge transfer resistance), which may be attributed to the desorption of the adsorbed film. The various corrosion parameters obtained are listed in Table 3.

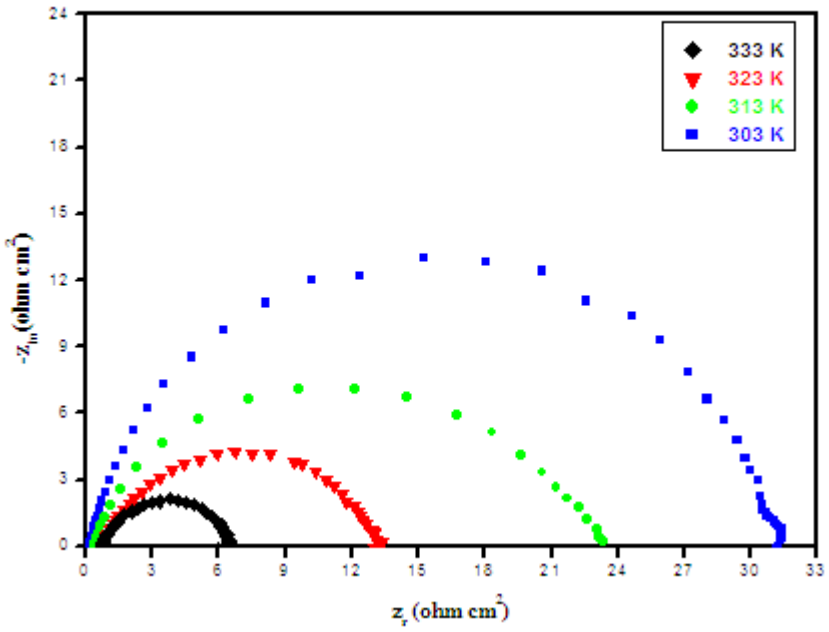

Figure 5 : Nyquist diagrams for carbon steel in 1.0 M HCl at different temperatures.

ISSN: 0975-8585

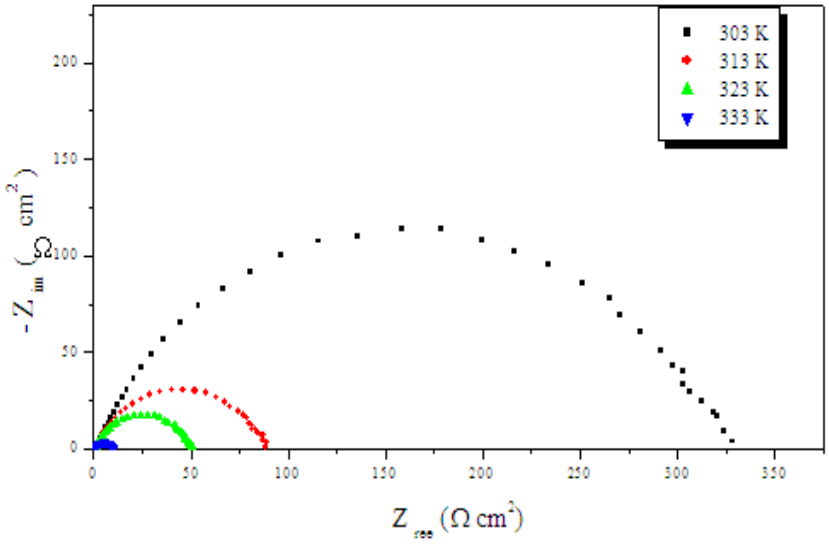

Figure 6 : Nyquist diagrams for carbon steel in 1.0 M HCl + 10^{-3}M of QIN2 at different temperatures.

Table 3 : EIS parameters and the corresponding inhibition efficiencies at various temperatures studied of carboon steel in 1.0 M HCl containing different concentrations of QIN2.

Inhibitor	Temp (K)	R_{ct} (Ω cm^2)	f_{max} (Hz)	C_{dl} (μF/cm^2)	η_z (%)
	303	31	128	40	----
Blank	313	27	40	147	----
	323	18	79	163	----
	333	6	158	168	----
	303	327 39.9	50	9.7	90.5
QIN2	313	80 168.6	50	39.8	66.2
	323	50 278.3	63	50.3	64.0
	333	11 1304.3	79	182.4	45.5

Values of R_{ct} were employed to calculate values of the corrosion current density (I_{corr}) at various temperatures in absence and presence of QIN2 using the following equation [37]:

$$I_{corr} = RT\left(zFR_{ct}\right)^{-1} \quad (6)$$

where R is the universal gas constant (R = 8.314 J mol^{-1} K^{-1}), T is the absolute temperature, z is the valence of iron (z = 2), F is the Faraday constant (F = 96 485 coulomb) and R_{ct} is the charge transfer resistance.

The activation energy of the corrosion process was calculated using the following equation:

$$I_{corr} = A\exp\left(-\frac{E_a}{RT}\right) \quad (7)$$

where E_a is the activation energy, A is the frequency factor, T is the absolute temperature, R is the gas constant and k is the rate of metal dissolution reaction which is directly related to corrosion current density [38] I_{corr}. Plotting Ln I_{corr} versus 1/T, the values of E_a can be calculated from the slopes of straight lines obtained from Fig. 7. The value of E_a obtained in 1.0 M HCl is equal to 50.45 kJ mol^{-1}. The value for the investigated compound is listed in Table 4. The activation energy is higher in the presence of additive than in its absence. This observation further supports the proposed physisorption mechanism. Unchanged or lower values of E_a in inhibited systems compared to the blank have been reported [39,40] to be indicative of chemisorption

mechanism, while higher values of E_a suggest a physical adsorption mechanism. This type of inhibitors retards the corrosion process at ordinary temperature [41] whereas the inhibition is considerably decreased at elevated temperature. Ebenso et al. [42] reported that for a chemical adsorption mechanism, inhibition efficiency increases with increase in temperature, whereas an increase in inhibition efficiency with decrease in temperature is suggestive of a physical adsorption mechanism.

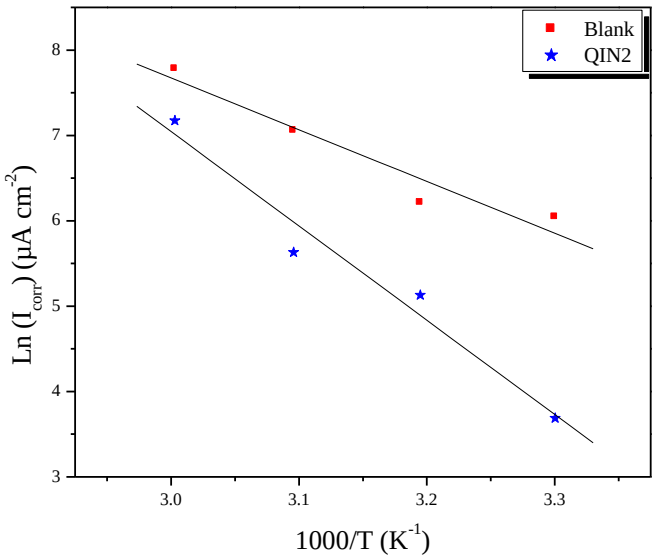

Figure 7: Arrhenius plots for carbon steel corrosion rates Ln (I_{corr}) versus 1/T in 1.0 M HCl in absence and in presence of optimum concentration of QIN2.

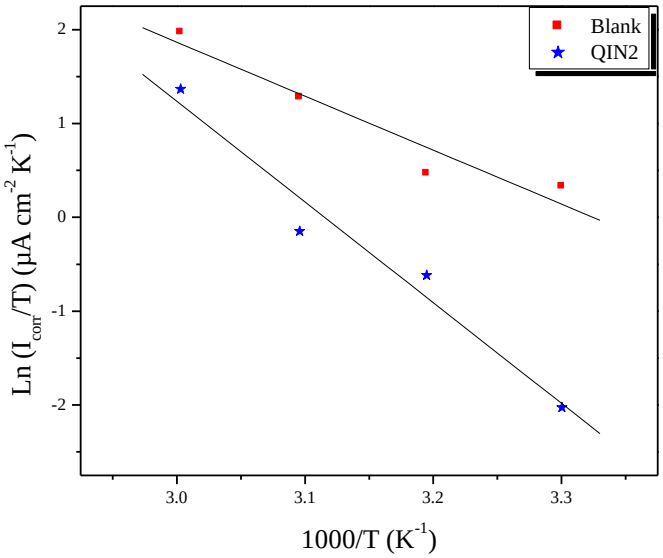

Figure 8: Transition-state plots for carbon steel corrosion rates Ln ($I_{cor}r/T$) versus 1/T in 1.0 M HCl in absence and in presence of optimum concentrations of QIN2.

Enthalpy and entropy of activation (ΔH_a, ΔS_a) were calculated from the transition state theory and listed in Table 4.

ISSN: 0975-8585

$$I_{corr} = \frac{RT}{Nh}\exp\left(\frac{\Delta S_a}{R}\right)\exp\left(\frac{\Delta H_a}{RT}\right) \quad (8)$$

where h is the Plank's constant and N is the Avogadro's number. Figure 8 shows a plot of Ln (I_{corr}/T) versus 1/T. A straight lines are obtained with a slope of (-ΔH_a/R) and an intercept of (Ln R/Nh + ΔS_a/R) from which the values of ΔH_a and ΔS_a were calculated.

The thermodynamic parameters (ΔH_a and ΔS_a) of the dissolution reaction of steel in 1.0 M HCl in the presence of QIN2 is higher than that of in the absence of inhibitor (blank). The positive signs of the enthalpies ΔH_a reflect the endothermic nature of the steel dissolution process and mean that the dissolution of steel is difficult [43]. In the presence of QIN2, the increase of ΔS_a reveals that an increase in disordering takes place on going from reactants to the activated complex [44].

Table 4: The values of activation parameters for carbon steel in 1.0 M HCl in the absence and presence of optimum concentration of QIN2.

	E_a (kJ mol^{-1})	ΔH_a (kJ mol^{-1})	ΔS_a (J mol^{-1} K^{-1})
Blank	50.45	47.81	-38.61
QIN2	91.86	89.22	80.40

Application of adsorption isotherm

Adsorption of the inhibitor molecule mainly depends upon charge and nature of the metal surface, electronic characteristics of the metal surface, adsorption of solvent and other ionic species, temperature and electrochemical potential at solution interface [45]. Inhibitor molecules undergo two types of adsorption with the metal surface. One is the physical adsorption (physisorption) resulting due to electrostatic attraction between inhibiting organic ions or dipoles and the electrically charged surface of metal and the other, chemical adsorption (chemisorption) resulting when charge sharing or charge transfer from adsorbates to the metal surface atoms in order to form a covalent type of bond. Chemical adsorption has free energy of adsorption and the activation energy higher than the physical adsorption [46]. The adsorption isotherm describes the adsorptive behaviour of organic compounds in order to know the adsorption mechanism. The most frequently used adsorption isotherms are Langmuir, Temkin, Frumkin and Freundlich isotherms. The correlation coefficient (R^2) was used to choose the isotherm that best fits the experimental data. To obtain the adsorption isotherm, the degree of surface coverage (θ) was using the equation:

$$\theta = \frac{R_{ct(inh)} - R_{ct}}{R_{ct(inh)}} \quad (9)$$

where R_{ct} and $R_{ct\ (inh)}$ were the values of polarization resistance in the absence and presence of inhibitor, respectively. Resistances transfer's charges were calculated using electrochemical impedance spectroscopy data.

By far the results were best fitted by Langmuir isotherm equation:

$$\frac{C_{inh}}{\theta} = \frac{1}{K_{ads}} + C_{inh} \quad (10)$$

where C_{inh} is the equilibrium inhibitor concentration, K_{ads} adsorptive equilibrium constant. Straight lines were obtained by plotting the graph of C_{inh} /θ vs. C_{inh} for this inhibitor at 303K (Figure 9). The regression coefficient is almost unity. These results suggest that the Langmuir adsorption isotherm model gives the best description of the adsorption behavior of QIN2 on the carbon steel surface. Equilibrium constant for the adsorption process is related to the standard free energy of adsorption by the following expression:

$$\Delta G^{\circ}_{ads} = -RTLn(55.5K_{ads}) \quad (11)$$

where R is gas constant and T is absolute temperature of experiment and the constant value of 55.5 is the concentration of water in solution in mol L^{-1}. The parameters calculated from the Langmuir adsorption isotherm model are reported in Table 5.

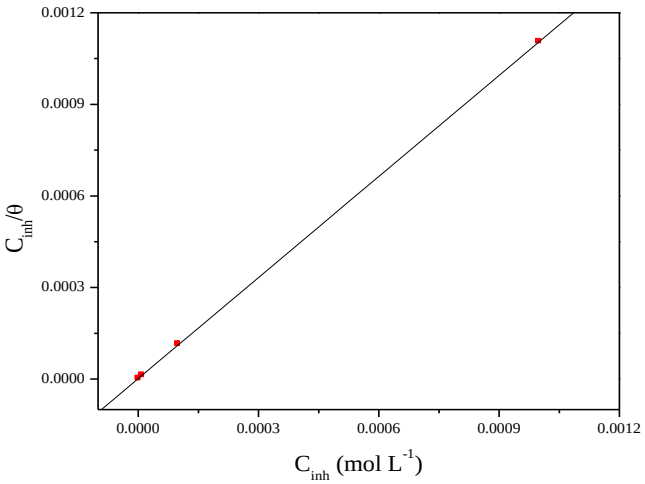

Figure 9: Langmuir adsorption isotherm plots for QIN2 at 303K.

Table 5. Langmuir adsorption parameters.

Inhibitor	Slope	K_{ads} (M^{-1})	R^2	ΔG°_{ads} (kJ/mol)
QIN2	1.1	644628.95	1.0	-43.81

The negative value of ΔG°_{ads} and the higher values of K_{ads} reveal the spontaneity of adsorption process and are characteristic of strong interaction and stability of the adsorbed layer with the steel surface.. Usually the values around -20kJ mol^{-1} or lower are consistent with physical adsorption, while those higher than -40kJ mol^{-1} involves chemical adsorption [47]. When charged species adsorbed on the metal surface, there is possibility of the columbic interaction between adsorbed cation and anion thereby causing increase in the ΔG°_{ads} even if no chemical bonds are formed [48]. In the present study, the calculated standard free energy of adsorption value is closer to -40 kJ mol^{-1} (Table 5). Therefore it can be concluded that the adsorption of the QIN2 on the carbon steel surface is more chemical than physical [49].

Quantum Chemical Calculations

The structure and electronic parameters were obtained by means of theoretical calculations using the computational methodologies of quantum chemistry. The optimized molecular structures and frontier molecular orbital density distribution of the studied molecule are shown in Figure 10. The calculated quantum chemical parameters such as E_{HOMO}, E_{LUMO}, $\Delta E_{LUMO-HOMO}$, dipole moments (μ) are listed in Table 6. The molecular structure of berberine shows that the molecules seems to adsorb on steel surface by sharing of electrons of the nitrogen and oxygen atoms with iron to form coordinated bonds and π-electron interactions of the aromatic rings.

ISSN: 0975-8585

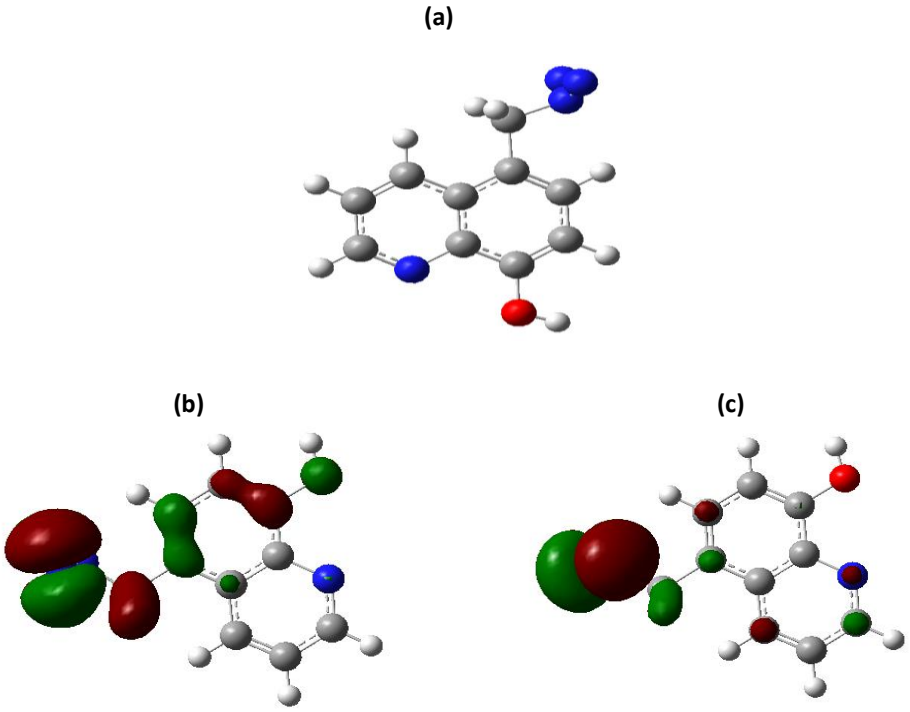

Figure 10 : (a) Optimized molecular structure (b) total charge density (c) HOMO (d) LUMO molecular orbital density distribution of QIN2.

Table 6 : Calculated quantum chemical parameters of QIN2.

Quantum parameters	QIN2
E_{HOMO} (eV)	-7.9457
E_{LUMO} (eV)	-5.8232
$\Delta E_{LUMO-HOMO}$	2.1225
Dipole Moment (μ)	0.9543

The value of highest occupied molecular orbital, E_{HOMO} indicates the tendency of the molecule to donate electrons through nitrogen and oxygen atoms to acceptor molecule with empty and low energy orbital. E_{LUMO} indicates the tendency of the molecule to accept electrons, with the trend often being that the lower E_{LUMO} is, the greater is the ability of that molecule to accept electrons [50,51]. The energy gap ΔE is an important parameter that is related to reactivity of the inhibitor molecule towards the metal surface. A high E_{H-L} is associated with a less tendency towards reactivity while a low E_{H-L} is an indication of a great tendency towards reactivity [52-55]. In this case, berberine showed a strong tendency towards reactivity. Polarity of a covalent bond (Dipole moment μ) can be understood by distribution of electrons in a molecule and large values of dipole moment μ favour the adsorption of inhibitor.

CONCLUSION

EIS experiments results reveal that the charge transfer resistances of the carbon steel electrode increases greatly while the double layer capacitance decreases with increasing the inhibitor concentration, implying that QIN2 inhibits through adsorption mechanism. Polarization curves indicate that inhibitor acts as a cathodic-type inhibitor. Thermodynamic calculation indicates that the adsorption of QIN2 follows well the Langmuir isotherm and the chemisorption is involved in the interaction between inhibitor and the carbon steel surface. Data obtained from quantum chemical calculations using DFT at the B3LYP/6-31G(d) level of theory were correlated to the inhibitive effect of QIN2. All measurements results obtained demonstrate that inhibitor has excellent inhibition properties for carbon steel in hydrochloric acid solution.

REFERENCES

[1] Singh A. K., Quraishi M. A., J. Mater. Environ. Sci. 1 (2010) 101.
[2] Prajila M., Sam J., Bincy J., Abraham J., J. Mater. Environ. Sci. 3 (2012) 1045.
[3] Naik U.J., Panchal V.A., Patel A.S., Shah N.K., J. Mater. Environ. Sci. 3 (2012) 935.
[4] Al Hamzi A.H., Zarrok H., Zarrouk A., Salghi R., Hammouti B., Al-Deyab S.S., Bouachrine M., Amine A., Guenoun F., Int. J. Electrochem. Sci. 8 (2013) 2586.
[5] Zarrouk A., Hammouti B., Zarrok H., Warad I., Bouachrine, M., Der Pharm. Chem. 3 (2011) 263.
[6] Ben Hmamou D., Salghi R., Zarrouk A., Messali M., Zarrok H., Errami M., Hammouti B., Bazzi L., Chakir A., Der Pharm. Chem. 4 (2012) 1496.
[7] Ghazoui A., Bencaht N., Al-Deyab S.S., Zarrouk A. , Hammouti B., Ramdani M., Guenbour M., Int. J. Electrochem. Sci. 8 (2013) 2272.
[8] Zarrouk A., Zarrok H., Salghi R., Bouroumane N., Hammouti B., Al-Deyab S.S., Touzani R., Int. J. Electrochem. Sci.7 (2012) 10215.
[9] Bendaha H., Zarrouk A., Aouniti A., Hammouti B., El Kadiri S., Salghi R., Touzani R., Phys. Chem. News. 64 (2012) 95.
[10] Rekkab S., Zarrok H., Salghi R., Zarrouk A., Bazzi L., Hammouti B., Kabouche Z., Touzani R., Zougagh M., J. Mater. Environ. Sci.3 (2012) 613.
[11] Zarrouk A., Hammouti B., Zarrok H., Bouachrine M., Khaled K.F., Al-Deyab S.S., Int. J. Electrochem. Sci.7 (2012) 89.
[12] Ghazoui A., Saddik R., Benchat N., Guenbour M., Hammouti B., Al-Deyab S.S., Zarrouk A., Int. J. Electrochem. Sci.7 (2012) 7080.
[13] Zarrok H., Mamari K.A., Zarrouk A., Salghi R., Hammouti B., Al-Deyab S.S., Essassi E.M., Bentiss F., Oudda H., Int. J. Electrochem. Sci. 7 (2012) 10338.
[14] Zarrok H., Zarrouk A., Salghi R., Ramli Y., Hammouti B., Assouag M., Essassi E.M., Oudda H., Taleb M., J. Chem. Pharm. Res.4 (2012) 5048.
[15] Zarrouk A., Hammouti B., Dafali A., Bentiss F., Ind. Eng. Chem. Res. 52 (2013) 2560.
[16] Zarrok H., Zarrouk A., Salghi R., Oudda H., Hammouti B., Assouag M., Taleb M., Ebn Touhami M., Bouachrine M., Boukhris S., J. Chem. Pharm. Res. 4 (2012) 5056.
[17] Zarrok H., Oudda H., El Midaoui A., Zarrouk A., Hammouti B., Ebn Touhami M., Attayibat A., Radi S., Touzani R., Res. Chem. Intermed. 38 (2012) 2051.
[18] Ghazoui A., Zarrouk A., Bencaht N., Salghi R., Assouag M., El Hezzat M., Guenbour A., Hammouti B., J. Chem. Pharm. Res.6 (2014) 704.
[19] Zarrok H., Zarrouk A., Salghi R., Ebn Touhami M., Oudda H., Hammouti B., Touir R., Bentiss F., Al-Deyab S.S., Int. J. Electrochem. Sci. 8 (2013) 6014.
[20] Zarrouk A., Zarrok H., Salghi R., Touir R., Hammouti B., Benchat N., Afrine L.L., Hannache H., El Hezzat M., Bouachrine M., J. Chem. Pharm. Res.5 (2013) 1482.
[21] Zarrok H., Zarrouk A., Salghi R., Assouag M., Hammouti B., Oudda H., Boukhris S., Al Deyab S.S., Warad I., Der Pharm. Lett. 5 (2013) 43.
[22] Ben Hmamou D., Aouad M.R., Salghi R., Zarrouk A., Assouag M., Benali O., Messali M., Zarrok H., Hammouti B., J. Chem. Pharm. Res. 4 (2012) 3498.
[23] Belayachi M., Serrar H., Zarrok H., El Assyry A., Zarrouk A., Oudda H., Boukhris S., Hammouti B., Ebenso Eno E., Geunbour A., Int. J. Electrochem. Sci. 10 (2015) 3010.
[24] Tayebi H., Bourazmi H., Himmi B., El Assyry A., Ramli Y., Zarrouk A., Geunbour A., Hammouti B., Ebenso Eno E., Der Pharm. Lett. 6(6) (2014) 20.
[25] Tayebi H., Bourazmi H., Himmi B., El Assyry A., Ramli Y., Zarrouk A., Geunbour A., Hammouti B., Der Pharm. Chem. 6(5) (2014) 220.
[26] Ma H., Chen S., Liu Z., Sun Y., J. Mol. Struct. (THEOCHEM). 774 (2006) 1922.
[27] Henrquez-Romn J.H., Padilla-Campos L., Pez M.A., Zagal J.H., Rubio M.A., Rangel C.M., Costamagna J., Crdenas-Jirn G., J. Mol. Struct. (THEOCHEM) 757 (2005) 17.
[28] Rodrguez-Valdez L.M., Martnez-Villafane A., Glossman-Mitnik D., J. Mol. Struct. (THEOCHEM). 713 (2005) 6570.
[29] Feng Y., Chen S., Guo W., Zhang Y., Liu G., J. Electroanal. Chem. 602 (2007) 115.
[30] Frisch M. J., Trucks G.W., Schlegel H.B., Scuseria G.E., Robb M.A., Cheeseman J.R., Montgomery J.A.,. Vreven Jr.T, Kudin K.N., Burant J.C., Millam J.M., Iyengar S.S., Tomasi J., Barone V., Mennucci B., Cossi M., Scalmani G., Rega N., Petersson G.A., Nakatsuji H., Hada M., Ehara M., Toyota K., Fukuda R., Hasegawa J., Ishida M., Nakajima T., Honda Y., Kitao O., Nakai H., Klene M., Li X., Knox J.E., Hratchian

H.P., Cross J.B., Bakken V., Adamo C., Jaramillo J., Gomperts R., Stratmann R.E., Yazyev O., Austin A. J., Cammi R., Pomelli C., Ochterski J.W., Ayala P.Y., Morokuma K., Voth G.A., Salvador P., Dannenberg J.J., Zakrzewski V.G., Dapprich S., Daniels A.D., Strain M.C., Farkas O., Malick D.K., Rabuck A.D., Raghavachari K., Foresman J.B., Ortiz J.V., Cui Q., Baboul A.G., Clifford S., Cioslowski J., Stefanov B.B., Liu G., Liashenko A., Piskorz P., Komaromi I., Martin R.L., Fox D.J., Keith T., Al-Laham M.A., Peng C.Y., Nanayakkara A., Challacombe M., Gill P.M. W., Johnson B., Chen W., Wong M.W., Gonzalez C., and Pople J. A., Gaussian 03, Revision E.01, Gaussian, Inc., Wallingford CT. 2004.

[31] Li W H., He Q., Pei C.L., Hou B.R., J. Appl. Electrochem., 38 (2008) 289.
[32] Ferreira E.S., Giacomelli C., Giacomelli F.C., Spinelli A., Mater. Chem. Phys. 83 (2004) 129.
[33] Behpour M., Ghoreishi S.M., Mohammadi N., Soltani N., Salavati-Niasari M., Corros. Sci.52 (2010) 4046.
[34] Larabi L., Harek Y., Traianel M., Mansri A., J. Appl. Electrochem.34 (2004) 833.
[35] El-Haddad M.N., Fouda A.S., Chem. Eng. Comm., 200 (2013) 1366.
[36] Trinstancho-Reyes J.L., Sanchez-Carrillo M., Sandoval-Jabalera R., Orozco-Carmona V.M., Almeraya-Calderon F., Chacon-Nava J.G., Gonzalez-Rodriguez J.G., Martínez-Villafane. Int. J. Electrochem. Sci.6 (2011) 419.
[37] ELaoufir Y., Bourazmi H., Serrar H., Zarrok H., Zarrouk A., Hammouti B., Guenbour A., Boukhriss S., and Oudda H., Der Pharm. Lett. 6 (2014) 526.
[38] Savithri B.V., Mayanna S., Indian J. Chem. Technol. 3 (1996) 256.
[39] Martinez S., Stern I., J. Appl. Electrochem. 31 (2001) 973.
[40] Abd El-Rehim S.S., Ibrahim M.A.M., Khaled K.F., Mater. Chem. Phys. 70 (2001) 268.
[41] Putilova I.K., Balezin S.A., Barasanik Y.P., Metallic Corrosion Inhibitors, Pergamon Press, Oxford (1960) 30.
[42] Ebenso E.E., Ekpe U.J., Ita B.I., Offiong O.E., Ibok U.J., Mater. Chem. Phys. 60 (1999) 79.
[43] Guan N.M., Xueming L., Fei L., Mater. Chem. Phys., 86 (2004) 59.
[44] Khamis E., Hosney A., El-Khodary S., Afinidad 52 (1995) 95.
[45] Singh A.K., Shukla S.K., Singh M., Quraishi M.A., Mater. Chem. Phys. 129 (2011) 68.
[46] Trabanelli G., in: F.Mansfeld (Ed.), Corrosion Mechanism, Mercel Dekker, New York. 2006.
[47] Umoren S.A., Obot I.B., Ebenso E.E., Okafor P.C., Ogbobe O., Oguzie E.E., Anti-Corros. Meth. Mat. 53 (2006) 277.
[48] Ozcan M., Solmaz R., Kardas G., Dehri I., Colloid Surf. A. 325 (2008) 57.
[49] Mallaiyaa K., Subramaniama R., Srikandana S.S., Gowria S., Rajasekaranb N., Selvaraj A., Electrochim. Acta. 56 (2011) 3857.
[50] Yadav D. K., Quraishi M. A., Ind. Eng. Chem. Res. 51 (2012) 14966.
[51] Yadav D. K., Quraishi M. A., Maiti B., Corros. Sci. 55 (2011) 254.
[52] Singh A., Quraishi M. A., Ebenso E. E., Int. J. Electrochem. Sci. 7 (2012) 12545.
[53] Kabanda M. M., Obot I. B., Ebenso Eno E., Int. J. Electrochem. Sci. 8 (2013) 10839.
[54] Gece G., Bilgic S., Corros. Sci. 51 (2009) 1876.
[55] Raja P. B., Qureshi A. K., Rahim A. A., Osman H., Awang K., Corros. Sci. 69 (2013) 292.